Monodisperse hydrogel microspheres by forced droplet formation in aqueous two-phase systems†

Iwona Ziemecka, Volkert van Steijn,* Ger J. M. Koper, Michel Rosso, Aurelie M. Brizard, Jan H. van Esch and Michiel T. Kreutzer

Received 4th September 2010, Accepted 10th November 2010
DOI: 10.1039/c0lc00375a

This paper presents a method to form micron-sized droplets in an aqueous two-phase system (ATPS) and to subsequently polymerize the droplets to produce hydrogel beads. Owing to the low interfacial tension in ATPS, droplets do not easily form spontaneously. We enforce the formation of drops by perturbing an otherwise stable jet that forms at the junction where the two aqueous streams meet. This is done by actuating a piezo-electric bending disc integrated in our device. The influence of forcing amplitude and frequency on jet breakup is described and related to the size of monodisperse droplets with a diameter in the range between 30 and 60 μm. Rapid on-chip polymerization of derivatized dextran inside the droplets created monodisperse hydrogel particles. This work shows how droplet-based microfluidics can be used in all-aqueous, surfactant-free, organic-solvent-free biocompatible two-phase environment.

Introduction

Aqueous two-phase systems (ATPS) consist of two immiscible aqueous solutions, which display a relatively low interfacial tension, typically of the order of 0.1 mN m^{-1}. The combination of an all-aqueous environment and the low interfacial tension makes these systems ideal for purification and extraction of biomolecules, such as proteins and enzymes as well as living cells, since they provide the mild conditions that do not denature or destabilize these biomaterials.[1,2] Examples of miniaturized extraction and purification using ATPS solvent combinations include fast and efficient separation of cells,[3] and partitioning and purification of proteins.[4] In all of these applications, the two phases flow in parallel, separated by a stable interface that does not collapse into droplets. In fact, as we will describe below, it is rather hard to produce droplets in these water-in-water systems in comparison to organic-water systems.

Our work is motivated by the desire to exploit, in an all-aqueous environment, all the advantages of droplet microfluidics, such as the use of droplets as vessels for synthesis or microcrystal formation and reactions at the interface to produce capsules. An important motivation to develop a droplet-based system is subsequent polymerization of the droplets to create hydrogel particles for delivery of drugs or cells, such as shown by Jain *et al.*,[5] who used conventional methods to create an ATPS emulsion of extracted biomaterials. For many aspects of pharmaceutical use of microgels, such as bio-distribution, uptake and release rate, the control of the droplet size and size distribution is crucial,[6] and microfluidic miniaturization can be an attractive route to generate monodisperse droplets and microgels.[7]

Delft University of Technology, Department of Chemical Engineering, Julianalaan 136, 2628 BW Delft, the Netherlands. E-mail: v.vansteijn@tudelft.nl

† Electronic supplementary information (ESI) available, see DOI: 10.1039/c0lc00375a

While the creation of droplets of high monodispersity is well-developed in microfluidic devices,[8] the low interfacial tension of ATPS limits the range of flow rates that allow spontaneous formation of droplets.[9,10] In short, for a given channel shape, viscosity ratio and flow ratio, the transition from a 'droplets' regime with monodisperse droplets to a less monodisperse 'jetting' regime, depends only on $Ca = \mu U/\gamma$, the ratio of viscous stresses ($\mu U/r$) to surface stresses (γ/r), with U the thread velocity, μ the thread viscosity, γ the interfacial tension and r the thread radius. In this context, the capillary number can be viewed as the ratio of a characteristic break-up time $t_{\mathrm{break}} \sim \mu r/\gamma$ and a flow time $t_{\mathrm{flow}} \sim r/U$. Now, a hundred-fold reduction in interfacial tension, not uncommon for aqueous two-phase systems in comparison with water-organics systems, requires a hundred-fold reduction in flow speed to still be able to form drops spontaneously. To maintain a wide range of practical flow rates, external forcing is needed to break up the otherwise stable thread. An example of such forcing was developed by Song and coworkers,[11,12] who generated droplets using electro-hydrodynamic forcing in a ionic ATPS with a interfacial tension of 5 mN m^{-1}. In their method, unidentified electrostatic forces, due to surface charges or bulk charges, are important during the formation of droplets.

In this work, we demonstrate an all-mechanical piezoelectric forcing (similar to piezoelectric on-demand droplet generation[13]) to create water-in-water droplets, where we control the size of the droplets independent of flow rates, and we polymerize these droplets on-chip. Interestingly, these droplets can be created for a wide range of flow conditions, well outside the 'droplet' regime for the situation without forcing. Using only mechanical actuation ensures that we are not constrained in our choice of ATPS phases by surface charge requirements, enabling us, in stead, to optimize our phase composition for gelation and/or polymerization. Of course, apart from the polymerization, the use of droplet microfluidics has all the well-known advantages such as selection, traffic control, sorting, rapid mixing and fast extraction

and mass transfer.[14] The ability to do so in a surfactant-free, organic-solvent-free all-aqueous system that is fully biocompatible is very attractive.

Materials

Our flow experiments are performed with the widely-used ATPS polyethyleneglycol (PEG, 10 w/w % in water, MW = 35 000)-dextran (dex, 20 w/w % in water, MW = 110 000) with an interfacial tension of 0.1 mN m^{-1}.[1,15] The viscosities were 58 mPas and 22 mPas for the dextran-rich phase and the PEG-rich phase, respectively. To create hydrogel particles, we synthesized a glycidyl methacrylate derivatized dextran (dex-GMA) using the recipe of Van Dijk-Wolthuis *et al.*[16] The degree of substitution in dextran was 15. For the polymerization experiments, one solution contained 10 w/w % PEG (MW = 35000) and 185 mg ml^{-1} ammonium peroxydisulfate (APS), and the other solution contained a saturated ($\approx$ 10 w/w %) dex-GMA in 0.22 M KCl and 2 v/v % of *N*,*N*,*N*′,*N*′-tetramethylethylenediamine (TEMED). PDMS devices were created using standard micromolding methods from SU-8-on-silicon masters. Piezoelectric bending discs (0.5 in. diameter, Piezo Systems, Cambridge, MA) were incorporated by glueing and subsequent casting of a second PDMS layer.[17] The rated bending displacement of these discs is $\pm$ 20 μm at $\pm$ 180 V.

Droplet formation

Our method for controlled droplet formation is illustrated in Fig. 1. We injected the dextran solution into the central channel of our device, and the PEG solution into the two side feeds. We first describe the flows that were found without actuating the piezoelectric disc. We found that dripping occurred for flow rates (q_{PEG}, q_{dex}) = (20, 2) μL h^{-1} and lower. For higher q_{PEG} and/or higher q_{dex}, jetting occurred. The flow rates that mark this transition between regimes in our 100 $\pm$ 5 $\times$ 85 $\pm$ 5 μm^2 channel agree within acceptable limits with those predicted by Guillot *et al.*[10] for a rectangular channel of 100 $\times$ 100 μm^2. The jet radius ranged from r_0 = 13 $\pm$ 1 μm for q_{PEG} = 60 μl h^{-1} to r_0 = 10 $\pm$ 1 μm for q_{PEG} = 84 μl h^{-1}. Note that these radii are small

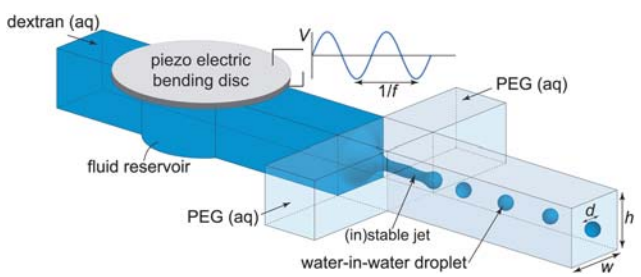

Fig. 1 Microfluidic device used for the controllable formation of microscopic-sized water-in-water droplets. Droplets are periodically released by perturbing the jet that forms at the junction where the stream of dextran solution and PEG solution meet. This is done by applying a sinusoidal AC voltage with amplitude V and frequency f to the piezo electric bending disc embedded in our device on top of the central channel. The bending disc squeezes the channel below it, accellerating the liquid inside it. For details on the design, see Fig. 1S in the Supplementary Information†.

compared to the width and height of the central channel. Stabilizing effects of confinement[10,18,19] are small for such thin jets.

Experimentally, we found that our threads were very stable, as shown in Fig. 2(a-c). Occasionally, we did observe spontaneous break up of the jet, relatively far ($\gg$ 1 cm) from the junction. The stability of our jet is remarkable, because theory predicts growth rates Re(ω) for initial disturbances of the thread interface $\tilde{r} = r_0 + \varepsilon e^{ikz + \omega t}$ of the order of 20 s^{-1}, suggesting that these threads should break up in less than 0.5 s, or, for the centerline flow speed U of 4 mm s^{-1}, within 2 mm for our experimental conditions. In agreement with this theoretical analysis, Guillot *et al.*[9] predicted fast break-up of threads with $2r_0/h < 0.5$ and stable threads for $2r_0/h > 0.5$, and confirmed this using glycerine/water in silicon oil. At present, we can only speculate about why our jets are so stable. We anticipate that particular properties of ATPS play a role. The present experiment involves more complex polymer solutions that exhibit more complex interfacial properties than pure liquids and hence the damping of fluctuations may be stronger than calculated for simple liquids. Finally, when the jet breaks far from the junction, that break up is always irregular, in agreement with the notion that it is caused by very slow amplification of noise in the system.

Forced drop formation

We now describe the flow regimes that were obtained by actuating the piezoelectric disc. When applying a sinusoidal AC voltage with frequency f and amplitude V to the piezo disc, the disc periodically bends up and down causing a disturbance in the flow. This disturbance, of much greater amplitude than the white-noise disturbances that cause unforced break-up, reproducibly breaks up the jet into droplets. Various break-up schemes were observed, depending mostly on the applied frequency. An example of breakup is shown in Fig. 2d-f: a corrugated jet (Fig. 2d) breaks up into elongated and corrugated droplets (Fig. 2e) and finally forms pairs of droplets further downstream (Fig. 2f).

Droplets were obtained for a much wider range of flow conditions using piezo-electric actuation than without. Fig. 3 shows a phase map of outer flow rate q_{PEG}, to inner flow rate q_{dex}. The dotted line indicates the theoretical transition from jetting to dripping that we confirmed for non-forcing flows. In comparison to unforced droplet formation, we could increase the flow rate of the inner stream with at least an order of magnitude, and the flow rate of the outer stream with almost two orders of magnitude, and still create monodisperse droplets.

Droplet size and monodispersity

In order to further characterize the effect of forcing, we studied droplet formation for voltages between V = 3 and 25 V and frequencies between f = 2 and 50 Hz for the flow conditions of Fig. 2, *i.e.* q_{PEG} = 60 μl h^{-1}, q_{dex} = 6 μl h^{-1}. A summary in the form of a map of voltages and frequencies presented in Fig. 4a shows under which conditions we obtained monodisperse and polydisperse droplets. Note that whether drop populations are monodisperse or polydisperse strongly depends on the actuation frequency, with a value of $f \approx$ 15 Hz that marks the transition,

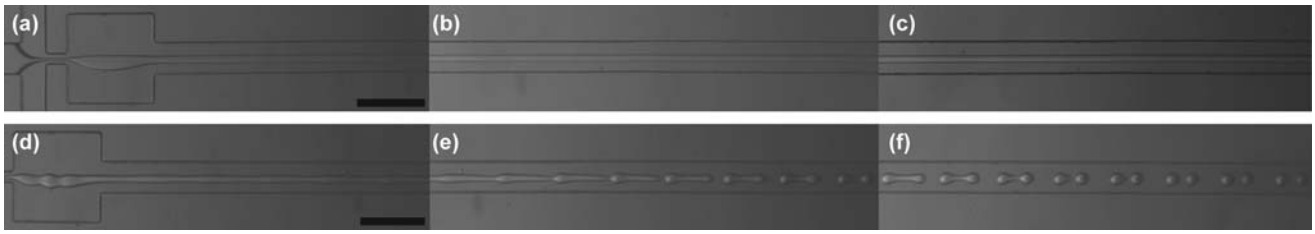

Fig. 2 (a-c): Jetting of the aqueous two-phase flow under steady feed conditions, *i.e.* without piezo-electrical actuation to induce oscillations. The jet is stable and does not break up at the location of focussing (a), not at 2 mm downstream (b), not at 5 mm downstream (c). (d-f): Formation of droplets from the jet in (a) by perturbing the jet through actuation of the piezo disc using a sinusoidal voltage with frequency $f = 20$ Hz and amplitude $V = 3$ V. At 2 mm downstream of the focussing (e), the jet breaks up, and the resulting long droplets break into two droplets at 5 mm downstream (f). See also the movie in Supplementary Information†. $q_{PEG} = 60\ \mu l\ h^{-1}$, $q_{dex} = 6\ \mu l\ h^{-1}$. Scale bars: 250 μm.

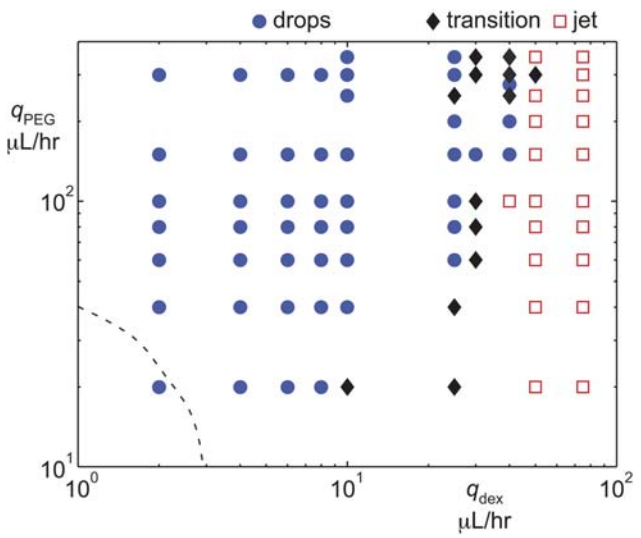

Fig. 3 Experimental phase map of inner flow rate *versus* outer flow rate, under piezoelectric actuation. The dashed line indicates the calculated drops-jet transition for unforced flow, based on ref. 10, which we confirmed in our experiments without forced oscillations.

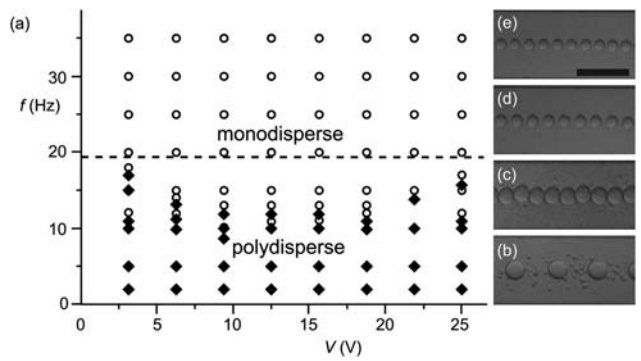

Fig. 4 (a) Influence of amplitude and frequency on the polydispersity of droplets. Solid diamonds: droplets with satellites and polydisperse droplets. Open circles: monodisperse droplets. (b-e) Droplets of dextran solution created in PEG solution by jet break-up with actuation frequencies of (b) 5 Hz (c) 10 Hz (d) 15 Hz (e) 20 Hz. For all experiments, $q_{PEG} = 60\ \mu l\ h^{-1}$, $q_{dex} = 6\ \mu l\ h^{-1}$, $V = 12.5$ V. Scale bar: 250 μm.

and only slightly on the amplitude of the voltage applied to the piezo disc.

Perhaps the most useful regime was obtained for frequencies between 20 and 50 Hz, because monodisperse droplets were reproducibly formed with diameters below 60 μm, and coefficients of variation below 10% (Fig. 4c and 4d). The upper bound of 50 Hz can be understood in terms of standard Rayleigh-Plateau theory.[20] This linear stability analysis of small disturbances predicts that dimensionless wavenumbers $kr_0 > 1$ are always stable and wavenumbers $kr_0 < 1$ are unstable. This result holds when extended to viscous two-fluid systems.[21] The wavenumber is related to the forcing frequency by $k = 2\pi f/U$. The frequency that corresponds to the cut-off wavenumber $kr_0 = 1$ reads $f = 50$ Hz for the values of $U = 4$ mm/*s* and $r_0 = 11$ μm. This theoretical value agrees with the observed maximum frequency at which break up is still observed.

Below $f = 10$ Hz, relatively large droplets formed directly at the junction. Depending on the frequency, the diameter of the droplets ranged between 70 and 150 μm. Although the size of the droplets was regular for fixed frequency and voltage, the droplets were accompanied by many small satellites with sizes between 10 and 40 μm as shown in Fig. 4b. The satellites form by the breakup of a very thin jet that forms just before the large drop pinches off, as the large droplet advances when the feed flow rate is at its minimum over the oscillation period. The number of satellites hereby reduced with increasing frequency.

For frequencies between 10 and 20 Hz, we observed both the formation of polydisperse droplets (Fig. 4c) as well as monodisperse droplets (Fig. 4d). It is interesting to observe the case of $f = 20$ Hz, which corresponds to an imposed wavelength that is exactly twice as long as the fastest growing wavelength, given by $kr_0 \approx 0.7$. Exciting the feed oscillations at twice this wavelength causes the jet to break up into droplets-pairs forming blobs, such as shown in Fig. 2(e-f). In this respect, the interaction of forcing frequency and natural frequency of the jet resembles the dynamics reported for the shearing of droplets from a side injection into a microchannel.[22] For the simpler case of an inviscid jet in vacuo, the effect of forcing has been extensively studied in relation to ink-jet printing.[23] Although these results cannot be directly translated to our viscous two-fluid system, they do show that the formation of satellite droplets may be suppressed or enhanced, depending on the relation between forcing wavenumber and fastest-growing wavenumber, which is qualitatively in agreement with our observations.

It is interesting to note that the location where the jet breaks up into droplets depends on the actuation frequency. For low frequencies, drops form directly at the junction. For frequencies around 10 Hz, drops are released from the jet a distance of a few mm downstream the junction. We observed that this distance increases with frequency. While it is tempting to relate this purely to hydrodynamic stability, another effect is also at play. We observe that as the frequency increases, the amplitude of the initial disturbances decreases. The cause of this damping may be in the piezoelectrics itself, or in the slow elastic response of the PDMS.[24]

To close the discussion on forced droplet formation, we show how drop size depends on the flow rates and the frequency of the sinusoidal voltage applied to the piezo disc. For the monodisperse regime shown in Fig. 4e, we plotted the drop diameter as a function of the frequency in Fig. 5 for five different flow rates of PEG solution in the range $q_{PEG} = 60$–$84\ \mu l\ h^{-1}$. The flow rate of the dextran solution was fixed at $q_{dex} = 6\ \mu l\ h^{-1}$. For fixed values of the flow rates, the graph shows that drop size can be effectively controlled by the frequency.

The frequency and flow-rate dependence on drop size can be understood from the simplest theoretical analysis based on conservation of mass. This analysis teaches that the rate at which the dextran solution flows into the jet, q_{dex}, equals the rate vf_d, at which it leaves the jet as drops, with v the drop volume and f_d the frequency at which drops are generated. We found experimentally that the frequency of drop formation is comparable to the actuation frequency of the piezo disc, $f = f_d$. In some cases (for instance that displayed in Fig. 2e) the drop initially released from the jet subsequently split up into two drops. For these cases, the volume v is divided over two equal-sized spherical drops with diameter d. In general, the volume v relates to the final drop diameter as $v = N\pi d^3/6$, where N is either one or two depending on whether this splitting up occurs. The drop diameter hence relates to the flow rate of dextran and the frequency applied to the piezo as $d = (6q_{dex}/N\pi f)^{1/3}$. The prediction of the drop diameter using this simplest model is shown in Fig. 5. The dashed line shows the prediction in case the drops initially released from the jet do not subsequently split up ($N = 1$), whereas the solid line shows the prediction in case split up does take place ($N = 2$). Despite its simplicity, this model adequately describes the experimental data.

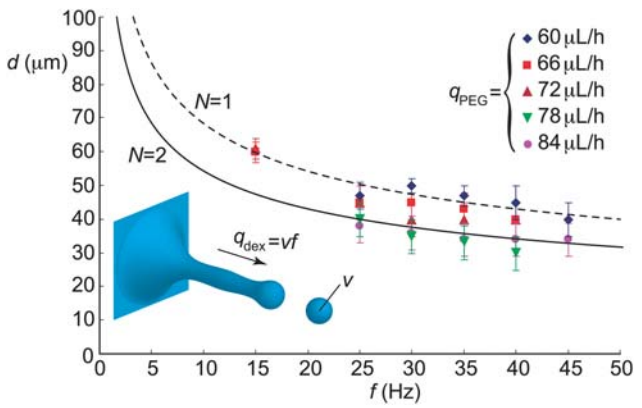

Fig. 5 Diameter of the droplets measured in the monodisperse regime indicated in Fig. 4e as a function of the actuation frequency of the piezo disc for five different flow rates of PEG solution and a fixed rate of flow of dextran solution of $q_{dex} = 6\ \mu l\ h^{-1}$. The dashed line is computed for the case that drops initially released from the jet do not subsequently split up into two equal-sized drops ($N = 1$), whereas the solid line shows the prediction in case split up occurs ($N = 2$).

Microgel formation

With the conditions to generate monodisperse droplets firmly established, we proceed to make hydrogel particles at those conditions. We synthesized a methacrylate derivatized dextran (dex-GMA), of which polymerization of the methacrylate groups leads to the formation of a cross-linked hydrogel in water.[16] The polymerization occurs *via* a radical mechanism, which was started by the introduction of the radical initiator ammonium peroxydisulfate *via* the PEG-rich stream. To accelerate the crosslinking, TEMED was added to the dex-GMA-rich phase. Upon contact of the two phases, APS diffuses to the dex-GMA-rich phase, where it reacts with TEMED to form the radicals that start the crosslinking and hence the gel formation (Fig. 6).

We could control the rate of polymerization through the concentration of TEMED. The polymerization, at high concentrations of TEMED, is fast enough to run to completion during the short residence time of the droplets in the PDMS microchip. We ran the reaction while actuating the piezoelectric disc ($V = 15$ V, $f = 35$ Hz), and found no difference in flow behavior with respect to the non-reactive solutions. We collected

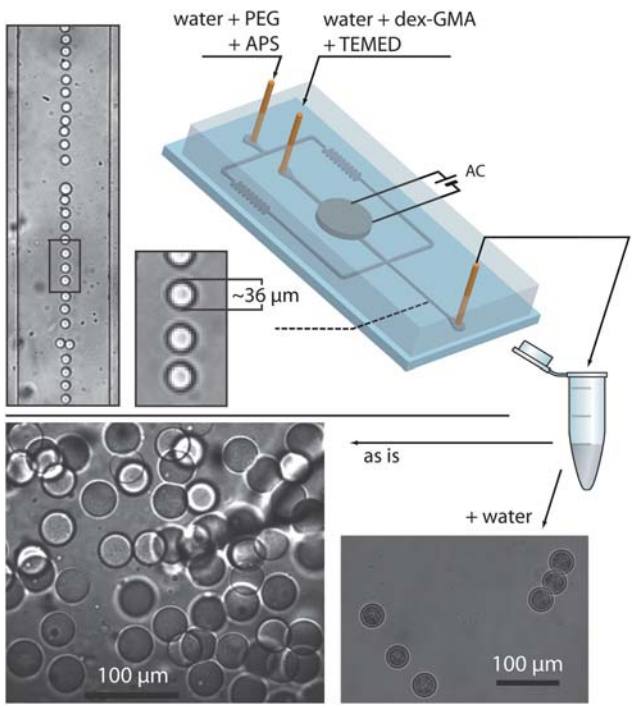

Fig. 6 Hydrogel microsphere formation for aqueous two-phase droplets. We introduce the functionalized dextran-rich phase and the initiator-containing PEG-rich phase and create monodisperse droplets on chip. Upon contact, the polymerization immediately starts. The effluent is collected and diluted, such that the two-phase system collapses. That single phase contains microgel bead of the same size as the generated droplets.

the microgel beads and subsequently dissolved them in water. This dilution destroys the two-phase system and causes unpolymerized dextran droplets to dissolve. After polymerization, however, stable beads remained, indicating that the cross-linking of the dextran-rich phase has occured. The size of these beads corresponded to the size of the monodisperse droplets produced in the microchannel ($d = 36 \pm 2$ μm).

The hydrogel beads were stable. We manipulated them with micropipettes and subjected them to vortex stirring, dried them on a glass slides and rehydrated them, recovering the round beads that we started with.

Conclusion and outlook

We presented a method to controllably and reproducibly form monodisperse water-in-water droplets with a diameter in the range between 30 to 60 μm, created by forcing oscillations in the feed with frequencies up to 50 Hz. Droplet sizes can be controlled by the actuation frequency of the piezo disc embedded in our device and the flow rates at which the aqueous solutions are supplied. We also demonstrated the possibility to produce monodisperse hydrogel beads from the same monodisperse droplets.

After demonstrating the potential of microfluidic ATPS in droplet microfluidics, it seems worthwhile to extend the applications to reactions, extractions and encapsulation in this all-aqueous environment. We believe the ability to use an aqueous phase to supply drops with chemicals, biomaterials and larger objects like cells and vesicles, or remove those from drops extends the potential of droplet microfluidics enormously.

Acknowledgements

The authors gratefully acknowledge NWO, NanoNed and COST Action D43 for financial support and Piet Droppert and Ben Norder for technical assistance.

References

1 P. A. Albertsson, *Nature*, 1956, **177**, 771–774; P. A. Albertsson, *Partitioning of Cell Particles and Macromolecules*, Wiley, New York, 1986.
2 H. Walter, G. Johansson and D. E. Brooks, *Anal. Biochem.*, 1991, **197**, 1–18.
3 M. Yamada, V. Kasim, M. Nakashima, E.J. and M. Seki, *Biotechnol. Bioeng.*, 2004, **88**, 489–494; K. H. Nam, W. J. Chang, H. Hong, S. M. Lim, K.D.I. and Y. M. Koo, *Biomed. Microdevices*, 2005, **7**, 189–195; J. R. SooHoo and G. M. Walker, *Biomed. Microdevices*, 2009, **11**, 323–329; M. Tsukamoto, S. Taira, S. Yamamura, Y. Morita, N. Nagatani, Y. Takamura and E. Tamiya, *Analyst*, 2009, **134**, 1994–1998.
4 G. Münchow, S. Hardt, J. P. Kutter and K. S. Drese, *Lab Chip*, 2007, **7**, 98–102; R. J. Meagher, Y. K. Light and A. K. Singh, *Lab Chip*, 2008, **8**, 527–532.
5 S. Jain, W. T. Yap and D. J. Irvine, *Biomacromolecules*, 2005, **6**, 2590–2600.
6 R. J. H. Stenekes, O. Franssen, E. M. G. van Bommel, D. J. A. Crommelin and W. E. Hennink, *Pharm. Res.*, 1998, **15**, 557–561.
7 E. Tumarkin and E. Kumacheva, *Chem. Soc. Rev.*, 2009, **38**, 2161–2168.
8 G. F. Christopher and S. L. Anna, *J. Phys. D: Appl. Phys.*, 2007, **40**, R319–R336; C. N. Baroud, F. Gallaire and R. Dangla, *Lab Chip*, 2010, **10**, 2032–2045.
9 P. Guillot, A. Colin, A. S. Utada and A. Ajdari, *Phys. Rev. Lett.*, 2007, **99**, 104502.
10 P. Guillot, A. Colin and A. Ajdari, *Phys. Rev. E: Stat., Nonlinear, Soft Matter Phys.*, 2008, **78**, 016307.
11 Y. S. Song, Y. H. Choi and D. H. Kim, *J. Chromatogr., A*, 2007, **1162**, 180–186.
12 Y. H. Choi, Y. S. Song and D. H. Kim, *J. Chromatogr., A*, 2010, **1217**, 3723–3728.
13 J. Xu and D. Attinger, *J. Micromech. Microeng.*, 2008, **18**, 065020; A. Bransky, N. Korin, M. Khoury and S. Levenberg, *Lab Chip*, 2009, **9**, 516–520.
14 B. G. De Geest, J. P. Urbanski, T. Thorsen, J. Demeester and S. C. De Smedt, *Langmuir*, 2005, **21**, 10275–10279; A. B. Theberge, F. Courtois, Y. Schaerli, M. Fischlechner, C. Abell, F. Hollfelder and W. T. S. Huck, *Ang. Chem. Int. Ed*, 2010, **49**, 2–25; A. Huebner, S. Sharma, M. Srisa–Art, F. Hollfelder, J. B. Edel and A. J. Demello, *Lab Chip*, 2008, **8**, 1244–1254; B. T. Kelly, J. C. Baret, V. Talyab and A. D. Griffiths, *Chem. Commun.*, 2007, 1773–1788; S.-Y. Tech, R. Lin, L.-H. Hung and A. P. Lee, *Lab Chip*, 2008, **8**, 198–220.
15 P. G. Mazzola, A. M. Lopes, F. A. Hasmann, A. F. Jozala, T. C. V. Penna, P. O. Magalhaes, C. O. Rangel-Yagui and A. Pessoa, *J. Chem. Technol. Biotechnol.*, 2008, **83**, 143–157.
16 W. N. E. van Dijk-Wolthuis, O. Franssen, H. Talsma, M. J. van Steenbergen, J. J. K. van den Bosch and W. E. Hennink, *Macromolecules*, 1995, **28**, 6317–6322.
17 M. T. Kreutzer, A. Günther and K. F. Jensen, *Anal. Chem.*, 2008, **80**, 1558–1567.
18 B. Dollet, W. van Hoeve, J. P. Raven, P. Marmottant and M. Versluis, *Phys. Rev. Lett.*, 2008, **100**, 034504.
19 K. J. Humphry, A. Ajdari, A. Fernández-Nieves, H. A. Stone and D. A. Weitz, *Phys. Rev. E: Stat., Nonlinear, Soft Matter Phys.*, 2009, **79**, 056310.
20 J. Eggers and E. Villermaux, *Rep. Prog. Phys.*, 2008, **71**, 036601.
21 H. A. Stone and M. P. Brenner, *J. Fluid Mech.*, 1996, **318**, 373–374.
22 H. Willaime, V. Barbier, L. Kloul, S. Maine and P. Tabeling, *Phys. Rev. Lett.*, 2006, **96**, 054501.
23 K. C. Chaudhary and L. Redekopp, *J. Fluid Mech.*, 1980, **96**, 257–274; K. C. Chaudhary and T. Maxworthy, *J. Fluid Mech.*, 1980, **96**, 275–286; K. C. Chaudhary and T. Maxworthy, *J. Fluid Mech.*, 1980, **96**, 287–297.
24 D. C. Leslie, C. J. Easley, E. Seker, J. M. Karlinsey, M. Utz, M. R. Begley and J. Landers, *Nat. Phys.*, 2009, **5**, 231–235.